Advanced Physics Lab SS19

Experiment: Short half lives

(conducted on: 2.-3.9.2019 with Krzysztof Bozek)

Erik Bode, Damian Lanzenstiel
(Group 103)

September 11, 2019

Abstract

In the short half life experiment, the half life of ^{57}Fe in the 14.4 keV state is measured with the delayed coincidence method. As the source, the Cobalt Isotope ^{57}Co is used.

Contents

1 Theory

1.1 Radioactive Decays

Radioactive Decays are spontaneous processes in which a unstable atomic nucleus transforms into another lighter one while emitting other particles. Typical forms of radioactive decay are the alpha $\beta+$ and the $\beta-$decay.

During the $\alpha-$decay a helium nucleus is emitted, reducing the atomic number by two. This form of decay is mainly found in heavy nucleus.

During the $\beta+$decay a proton transforms into a neutron and emits a positron as well as a electron-neutrino, reducing the atomic number by one.

$$p \to n + e^+ + v_e$$

On the other hand the $\beta-$decay is the reverse. It transforms a neutron into a proton and emits a electron and a electron-antineutrino. This decay increases the atomic number.

$$n \to p + e^- + \bar{v}_e$$

Another for the experiment important decay is the Electron Capture (EC) or $\epsilon-$decay. This one is similar to the $\beta+$decay since it also transforms a proton into a neutron. The difference being, that here the proton captures a electron to transform. The emitted particle is a electron-neutrino.

$$p + e^- \to n + \bar{v}_e$$

The captured electron is mostly from the K-shell while the resulting hole in the shell is filled by electrons from the L-shell. The remaining energy is either emitted through a X-ray photon or a Auger-electron. An Auger-electron is an electron that got the energy of an electron filling the vacancy left by electron in a lower state. The Auger-electron is therefore ejected.

These decays are often accompanied by a $\gamma-$decays. When a decay occurs the daughter nucleus is mostly left in an exited state. It then decays into the ground state emitting γ-rays.

Another Process similar to the γ-decay is the internal conversion (IC). Here the energy of a decay into a lower state is transmitted without radiation. That means no real photon is created to transport the energy. The energy is directly absorbed by another electron from the shell and ejected. The hole is filled similar to the one of EC by X-ray or Auger-electrons.

1.2 Interaction between Matter and $\gamma-$Photons

When $\gamma-$photons and matter interact this happens mostly in 3 different ways depending on the atomic number of the atoms in the matter, as well as the Energy E_γ of the photons.

1. Photoelectric effect:
   The photoelectric effect happens when a photon is absorbed by an electron inside the matter. The energy carried by the photon is turned into kinetic energy and frees the electron. The vacancy is filled by electrons from higher shells and the energy is emitted by an Auger-electron or X-ray.
   This effect appears mostly by $E_\gamma < 200\,\text{keV}$ and an atomic number around 50.

2. Compton scattering:
   Unlike the photoelectric effect the photons are not absorbed by the electrons in the matter. They give up a part of their energy and scatter at the electron.
   The Compton scattering happens by Energies in the range of $200\,\text{keV} < E_\gamma < 5\,\text{MeV}$ and a atomic number similar to the photoelectric effect.

3. Pair Production:
   Pair production is an effect that appears by an energy E_γ over the critical one of $1.022\,\text{MeV}$. When a γ-quantum gets into the electromagnetic field of a nucleus or electron it can be converted into an electron positron pair.
   $$\gamma \to e^- + e^+$$

   To create this pair the energy of $1.022\,\text{MeV}$ is needed this is also the reason the pair production can't happen if the photon has less energy. The remaining energy is given to the nucleus. The positron annihilates with an electron shortly after it's creation into two γ-rays with each half $0.511\,\text{MeV}$.

1.3 Energy Spectrum

In the energy spectrum are a few areas of interest.

First of all their are the Photo-peaks. These are peaks which come into being when a photon gives its whole energy to the detector. This will happen during a photoelectric effect if the emitted x-Ray or auger electron also gets absorbed.

Another region of interest (ROI) could be the Escape-peak. Here the x-Ray emitted by an exited state dropping to back to the ground state leaves the detector without interaction. That means the Escape-peak will be shifted by the amount of energy that left the detector.

The next point is the Compton edge and spectrum. If the emitted photon only interacts with the detector only by Compton scattering, and leaves the detector only a part of the energy will be deposed. This energy will form the Compton-spectrum. For a scattering angle of 180 the maximum amount of energy will be absorbed. This energy symbols the abrupt end of this spectrum and is called the Compton-edge.

Last but not least there is the Backscatter-peak happens through photons that get scattered at material outside of the detector and find their way back in where they get absorbed. That way they lose some energy depending on the material. This is way the peak is shifted by this amount from the position of the Photo-peak.
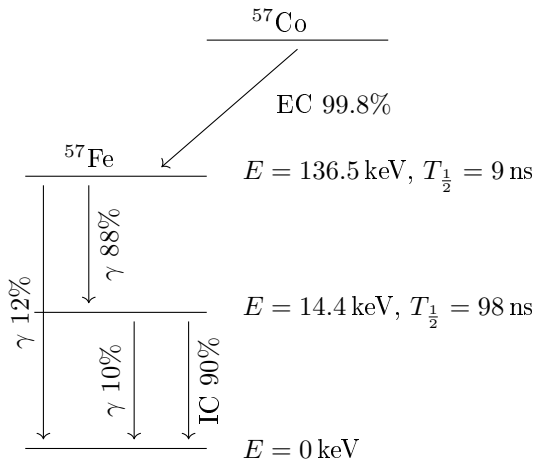
1.4 Methodology

Figure 1: Decay scheme for the cobalt isotope ^{57}Co into ^{57}Fe used into the experiment to measure the half-life of the 14.4 keV state of the Iron isotope.

To measure the half-life of ^{57}Fe we use the decay of the ^{57}Co Isotope (see figure 1) ^{57}Co decays by EC into an exited state of ^{57}Fe. At this point it can either decay directly to the ground state emitting a γ-photon.

The more likely case with 88% is, that it first goes to the wanted state of 14.4 keV by emitting a γ−ray. From this state it again has two options. With a 90% probability we have an IC which we can't detect but there is also a 10% chance that a γ−decay takes place.

To measure the half-life it makes sense to use the method of delayed coincidence. For this kind of measurement we need to measure the time Δt it takes for the 14.4 keV state to decay. The γ-photons connected to this state can be used to track the creation and the decay of the measured state and with that our time Δt. This time is of interest since like the radioactive decay which is a stochastic process, it follows the eq.1. [2]

$$N(t) = N(0)e^{\frac{t}{\tau}} = N(0) * 2^{t/T_{\frac{1}{2}}} \tag{1}$$

- $N(t)$: Number of existing nucleus at a given time.

- $N(0)$: Number of nucleus at the time zero.

- τ: Mean life time of the decaying quantity.

- $T_{\frac{1}{2}}$: Half-life of the decaying quantity.

With that the amount of measured decays at certain times Δt the half-life can be calculated. A problem that appears for the used decay is the rarity of the γ-ray with 14.4 keV. This one has only a 10% chance of appearing and stopping our measurement. That would lead to a long dead time in which no new

measurement can be taken. The problem is easily solved by using the rarer signal as the start of the measurement and stopping it with the 122 keV photon. Since there are also random coincidences which will distort the measurement a background measurement has to be made. This one can be subtracted from the real measurement.

1.5 γ-Ray Detection

To detect the γ-rays two scintillators which react to the γ-photons exhibiting scintillation will be used. This again can be detected by a photomultiplier tube (PMT) and converts them into an electric pulse. As scintillators organic and inorganic ones can be used. The main difference being the decay time of the emission centers and the luminous efficiency. If the half-life is bigger than 10^{-9} s inorganic Naj(Tl)-scintillators are the choice since they have the higher luminous efficiency. For shorter times organic ones have to be used because of the shorter decay time.
For this experiment inorganic ones can still be utilized. The light from emitted can by light transmission bars to the PMTs. That way the loss will be minimized.
The PMT is used to generate an electric signal by using the photoelectric effect. The pulse is increased by using increasing the velocity of the electrons freed by the photons and using them to free even more electrons at the dynode. This process will be repeated till a useful signal is produced.

2 Experimental Setup

2.1 Energy Spectra

In the first part of the experiment the energy spectrum of ^{57}Co and ^{241}Am are measured. For this the setup in figure 2 is used. Here the signals from the scintillator gets converted into an electric pulse and the Preamplifier (PA) provides a measurable signal. In the Main Amplifier (MA) the signal gets further amplified with low-noise. After this the pulse gets to the Multichannel Amplifier were it gets registered depending on the amplitude of the signal into a channel. This way a histogram can be formed. The output of the MA is for this measurement unipolar because only the amplitude of the signal is of importance. The spectra are needed to calibrate the MCA since a connection between known energies and the channel number can be made.[1]

Figure 2: Setup for the measurement of energy spectra with the MCA. [1]

2.2 SCA Thresholds

In the next part of the experiment the energy windows for the Single Channel Analyser (SCA) have to be set. One have to be set to filter out 122.1 keV photons and the other one to filter the 14.4 keV ones out. For this the setup in figure 3 is used. The Linear Gate in the setup only lets through a signal only when two signals one at the input and on at the enabler arrive at the same time. That way we can precisely set the energy window at the SCA. By moving the upper and lower threshold of the window, pulses with amplitudes outside of the thresholds are stopped and with that the other signal is stopped at the gate as well. By watching the histogram created by the MCA the thresholds can be set to the correct energy levels. [1]
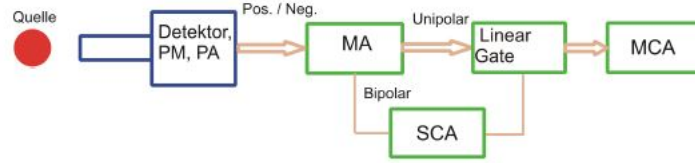
Figure 3: Setup for the calibration of the energy windows to filter out the photons with correct energies. [1]

2.3 Delayed Coincidences

The setup in figure 4 is used to make the measurement of delayed coincidences. In this setup the two sides of the detectors are connected to the calibrated SCAs. The TAC takes a start and a stop signal and creates a signal with an amplitude proportional to the time between the input signals. Since the measurement is started with the later $14.4\,\mathrm{keV}$ photon the earlier photon needs to be delayed so that it can stop the measurement.[1]
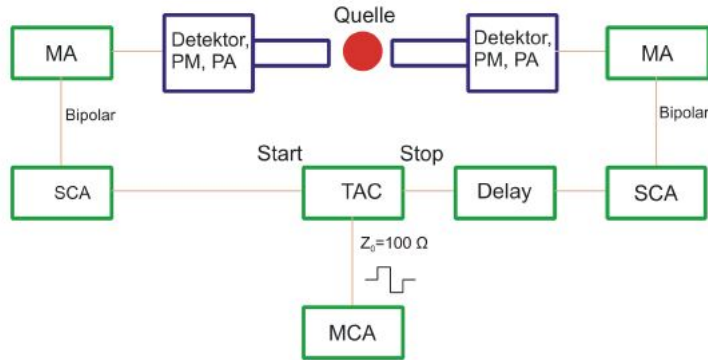
Figure 4: Setup for the measurement with the method of delayed coincidences. [1]

2.4 TAC Calibration

Last but not least the TAC needs to be calibrated. For this the setup in figure 5 will be used. With this the constant of proportionality between the delay and the channel number of the MCA can be calculated. [1]
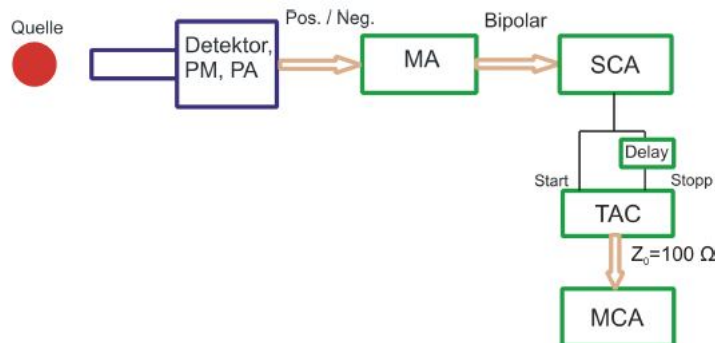
Figure 5: Setup for the calibration of the TAC. [1]

3   Conduction of the Experiment

First of all the ^{141}Am isotope was put into the detector. Directly after the PA and the MA were connected to an oscilloscope. Here the signals of both could be compared like in figure **??**.

After this the MCA was connected like in figure 2. The MCA was also connected to the interface from which the measurement of the energy spectra can be started. With the ^{141}Am source one measurement with each scintillator was made. These can be used to make the energy calibration of the MCA.

After this measurement the ^{141}Am source was switched with the ^{57}Co source. Here four different spectra were taken, two for both detectors with different sides of the sample. With these information the best combination of side of the sample and scintillator was chosen for the different energies. With this set the calibration of the energy windows could be started. For this the layout in figure 3 was used. First the window was opened completely so the whole spectrum, which was measured before could be seen. Than the thresholds at the SCA were slowly adjusted so that only one peak of the needed energy could be seen on the computer. After both SCAs were configured the actual measurement seen in figure 4 was set up. For the delay we choose the highest of 196 ns to get as much of the exponential curve as possible. After running a test the main measurement was started with a timer of 15 hours. Since the measured spectrum had a big part with only random coincidences this can be used instead of another measurement for the random coincidences. At last the calibration for the TAC was done by using the setup of figure 5. Here different delays were set and the corresponding channel were noted.

4   Analysis

4.1   Energy Calibration

To calibrate the MCA the decay of the Americium is used since it has clear visible Photo-peaks with known energies. To get the position of the peaks three Gaussian peaks are fitted on the curves. For the fits the python package `scipy.optimize.curve_fit`[3] was used. For the 59.5 keV peak the equation 2 was used.

$$f(x) = Ae^{-\frac{x-\mu}{2\sigma^2}} + C \tag{2}$$

In figure **??** the two peaks can be seen. For the other two peaks which are pushed together, two added Gaussian curves in the form of equation 3 are used.

$$f(x) = Ae^{-\frac{x-\mu}{2\sigma^2}} + A_2 e^{-\frac{x-\mu_2}{2\sigma_2^2}} + C \tag{3}$$

These fits are given in figure 13 and 14. With the value of the three different μ we get the position of the maximums.

	59.5 keV	33.2 keV	26.3 keV
Right Scintillator μ	120.61 ± 0.23	191.25 ± 0.29	419.53 ± 0.023
Left Scintillator μ	123.92 ± 0.30	179.91 ± 0.28	372.83 ± 0.022

Table 1: Positions of the different energy peaks of the right and left scintillator.

These values can be plotted as a line which gives for every channel the corresponding energy. R^2 is the coefficient of determinate and n the channel number.

$$f(x)_{Right} = (0.1120 \pm 0.0033)\,^{\text{keV}}/n * x + (12.3 \pm 0.9)\,\text{keV} \qquad R^2 = 0.9991 \tag{4}$$

$$f(x)_{Left} = (0.1341 \pm 0.0023)\,^{\text{keV}}/n * x + (9.4 \pm 0.5)\,\text{keV} \qquad R^2 = 0.9996 \tag{5}$$

The fits can be seen in figure 11.

4.2   Analysis of the Signal Shapes

In figure 6 we see the signal coming from the PA output of the detector. The signal reaches almost instantaneously its peak and than drops slowly down to the ground level. If we compare this signals with the one coming from the MA we can see that they are more Gaussian like and the beginning of the
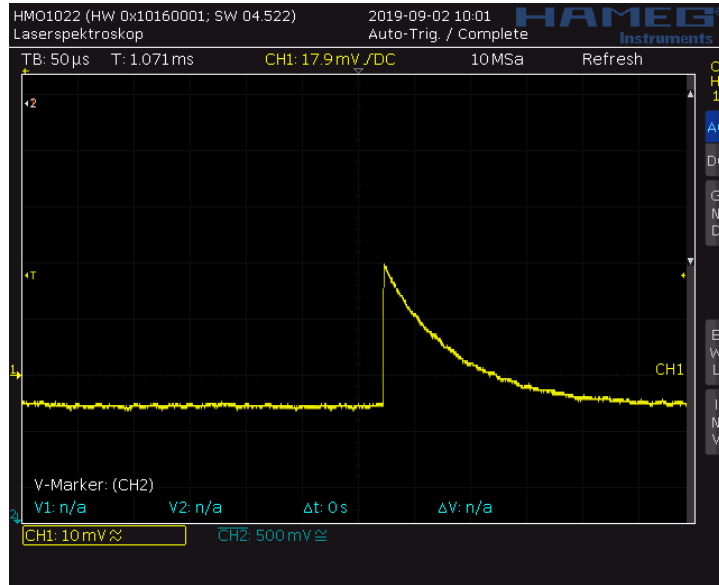
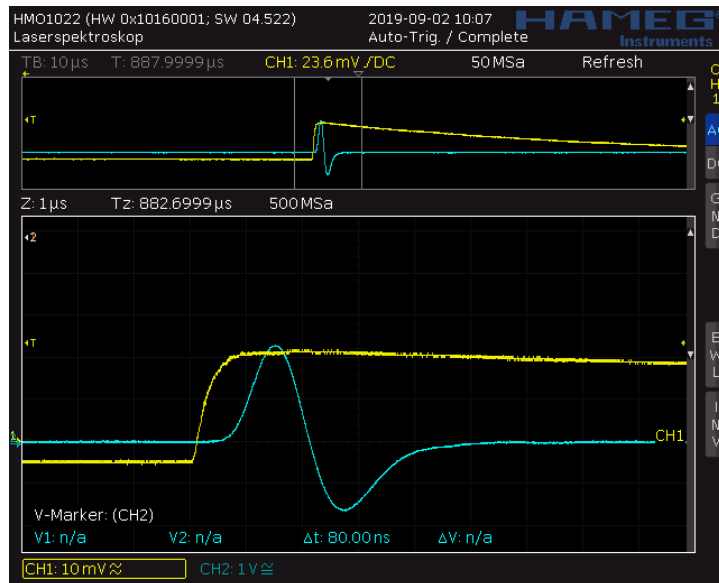Figure 6: Signal of the PA measured with an oscilloscope.

Figure 7: Bipolar signal output of the MA compared to the signal coming from the PA. Measured with an oscilloscope. In yellow the signal of the PA. In Blue the signal of the MA.
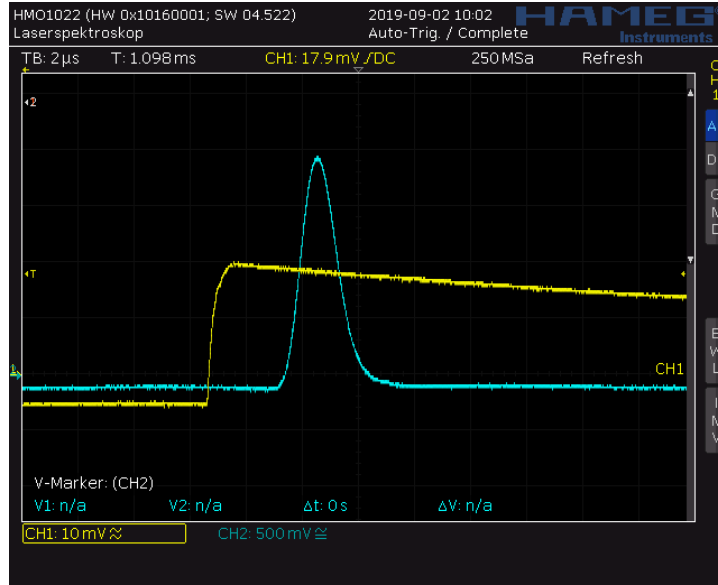
Figure 8: Unipolar signal output of the MA compared to the signal coming from the PA. Measured with an oscilloscope. In yellow the signal of the PA. In Blue the signal of the MA.

signal is a bit shifted to the left. In figure 7 the maximum of the blue signal is only a bit higher than the signal of the PA but its obvious that we have a bipolar signal. It is also notable that the ground level of the MA is higher than the one of the PA. In figure 8 this is the same but we see that the maximum amplitude of the MA signal is much higher than the one of the PA and we have a bell shaped signal. Comparing right and left slope of the MA curves with each other we notice that here the left side has a bit sharper increase than the right side of the signal.

4.3 Analysis of the Energy Spectra

4.3.1 Americium Spectra

Looking at figure 12 we see that the two spectra are shifted against each other. It is likely that the scintillators have a different amplification which causes this shift. Because of this two different energy calibrations are needed.

Looking at the spectra we see mainly the three Photo-peaks of the decays we expect. The positions of other regions of interest (ROI) are noted in the table 2 To calculate the Escape Peak 28 keV were deducted

ROI	Expected Energy [keV]	Right Channel	Left Channel
Escape Peak of 59.5 keV	31.5	171 ± 10	165 ± 5
Escape Peak of 26.3 keV	-	-	-
Escape Peak of 33.2 keV	-	-	-
Compton Edge of 59.5 keV	11.23	-10 ± 8	14 ± 4
Compton Edge of 26.3 keV	2.45	-88 ± 9	-52 ± 4
Compton Edge of 33.2 keV	3.82	-76 ± 9	-42 ± 4

Table 2: Points of interest for the scintillators. To calculate the channel equation 4 for the right side and equation 5 for the left side is used. The equations are tuned for the different scintillators. Left Channel gives the positions of the two spectra of the left one. The column Right Channel gives the position for the right scintillator. The - means that the peak ether cant exist in the spectrum.

from the Photo-peaks energy since this is the energy between the K and L shall in this experiment. To calculate the energy of the Compton edge equation 6 was used.

$$E_{Compton} = E_{\text{Photon}} - \frac{E_{\text{Photon}}}{1 + \frac{2E_{\text{Photon}}}{E_{\text{Electron}}}} \tag{6}$$

8

Looking at these it can be expected to see an Escape Peak of the 59.5 keV peak and its Compton Edge. The Reason we don't see them is that our Escape Peak is overshadowed by the Photo Peak of our 33.2 keV Photon. For the Compton Edge its possible that our energies are to low for it to happen often enough that it would get visible since the Compton scattering happens mostly in the range of 200 keV to 5 MeV.

4.3.2 Cobalt Spectra

The cobalt spectra was measured four times and all four spectra can be seen in figure 9. Since the two spectra where the screw of the source was turned to the scintillator are much lower, these are separate in figure 10. Looking at the figures we can clearly see the 122.1 keV peaks. But in this peak there is also hidden the in theory smaller, duo to its lower probability, 136.5 keV peak. These are similar to the 26.3 keV and 33.2 keV peaks very close to each other. That's why the 136.5 keV Photo-peak is hidden in the big peak at the right side of the spectrum. It is also visible that depending on which sides of detector are here also shifted against each other. Notable as well is that there is a smaller shift depending on the side of the source. So the spectra measured with the screw side are a bit sifted to the left. In the table 3 the positions of certain expected regions are listed. The Compton Edge was calculated like in the Americium Spectrum before with equation 6.

ROIs	Expected Energy [keV]	Right Channel	Left Channel
Photo Peak of 136.5 keV	136.5	1107 ± 34	947 ± 17
Photo Peak of 122.1 keV	122.1	979 ± 30	840 ± 15
Photo Peak of 14.4 keV	14.4	18 ± 8	37 ± 4
Escape Peak of 136.5 keV	108.5	857 ± 26	738 ± 13
Escape Peak of 122.1 keV	94.1	729 ± 23	631 ± 12
Escape Peak of 14.4 keV	-	-	-
Compton Edge of 136.5 keV	11.23	313 ± 12	284 ± 6
Compton Edge of 122.1 keV	2.45	242 ± 11	224 ± 6
Compton Edge of 14.4 keV	3.82	-103 ± 9	-64 ± 5

Table 3: Expected positions of certain regions of interest in the cobalt spectrum. The channels were calculated out of the expected energies with the equations 5 and 4. The equations are tuned for the different scintillators. Left Channel gives the positions of the two spectra of the left one. The column Right Channel gives the position for the right scintillator. The - means that the peak ether cant exist in the spectrum.

Comparing the expected positions to the measured ones we see that these don't align to well. For example is the expected position of the 136 keV Photo Peak outside of our measured spectrum for the right scintillator while left one is at the position were we see the right peak in figure 9. Since it is unlikely that those peaks in the figure aren't the 122.1 keV peaks its possible that our calibration isn't very precise. The reason for this may be that there is a systematic error that wasn't considered which shifted the cobalt spectra or the americium spectra into one direction. If we consider this its very likely that the peaks closest to the 122.1 keV peaks are the 108.5 keV and 94.1 keV Escape Peaks because they are expected to be quite close to the main peaks. The Compton Edge is very likely not visible since the chance for Compton scattering is to low because of the low energy levels. At channel number 200 we see a peak which might be a backscatter peak which originates from photon that lost energy outside of the scintillator can got back were they were absorbed. The little increase after this is what we expected to be the area of the 14.4 keV peak. Since the calibration isn't reliable we can't be sure of it. The low count rates at this part of the spectrum might come from the increase in the lower level discriminator (LLD) value during the experiment. Since there was an unrealistic high count rate at the lower energy level it was increased and it also affects the count rate of the region were the 14.4 keV photon is expected to be. The high count rate probably comes from electronics.
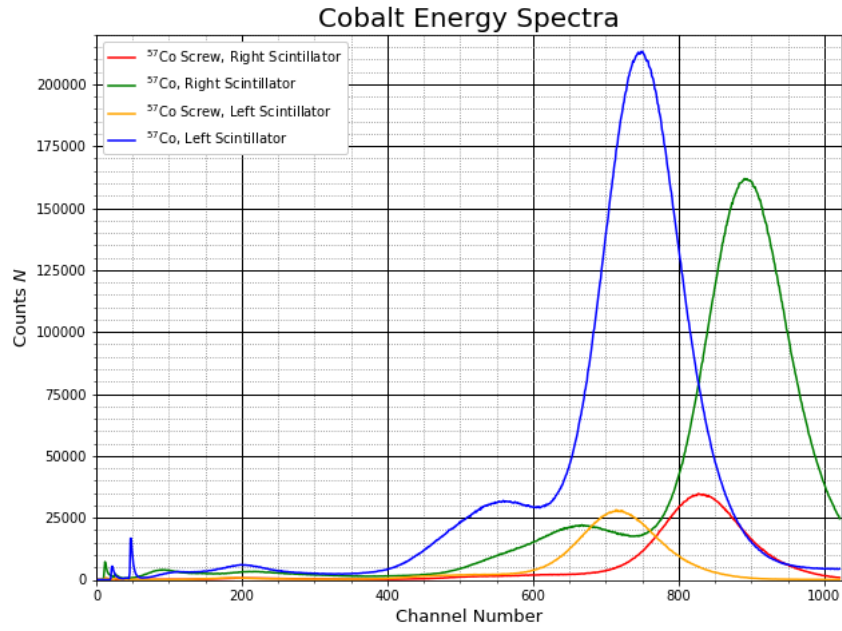
Figure 9: Energy Spectra of Cobalt with both sides of the detector and sides of the source.
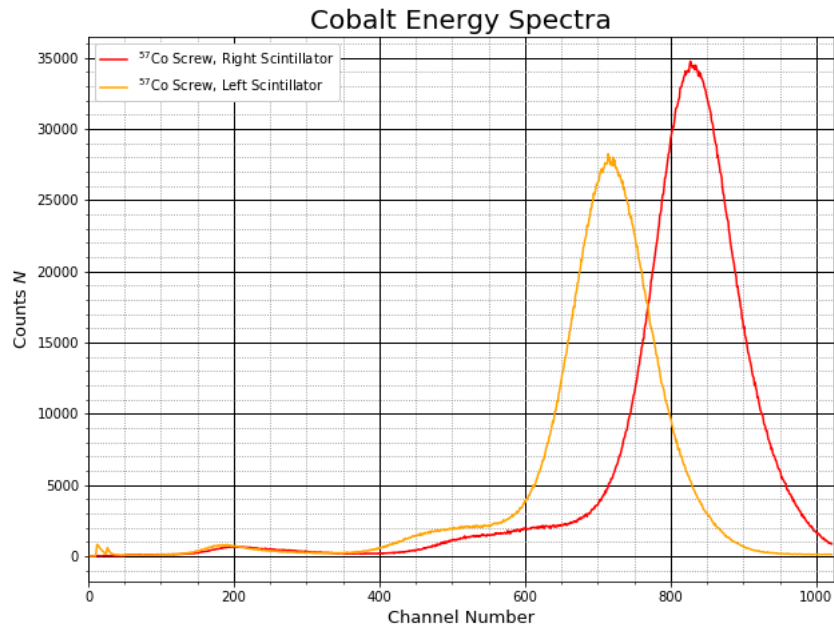

Figure 10: Energy Spectra of Cobalt of the two less visible peaks duo to lower radiation from the side of the screw.
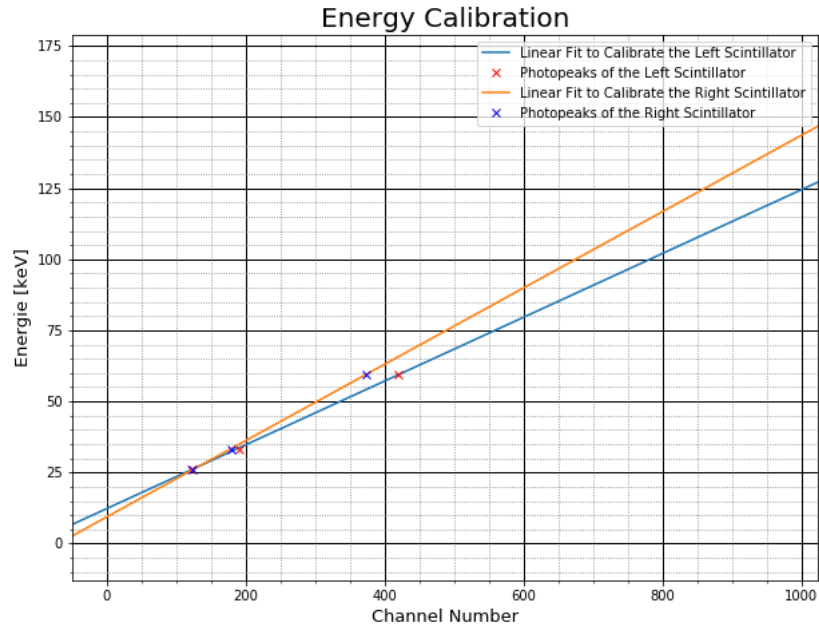
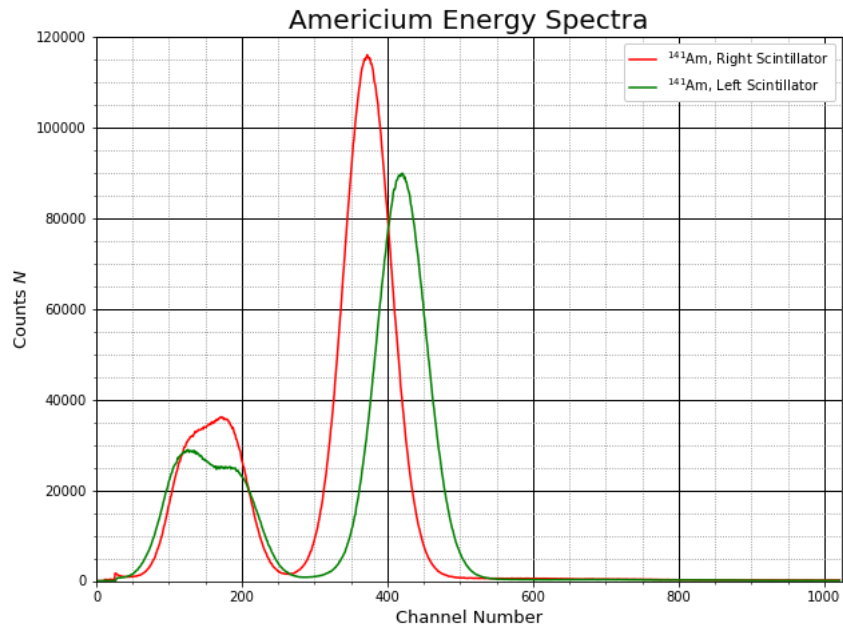Figure 11: Calibration curves for the energy calibrations.

Figure 12: Measured Americium Energy Spectra. The green curve is the measurement with the left scintillator while the red one is the scintillator of the right detector side.
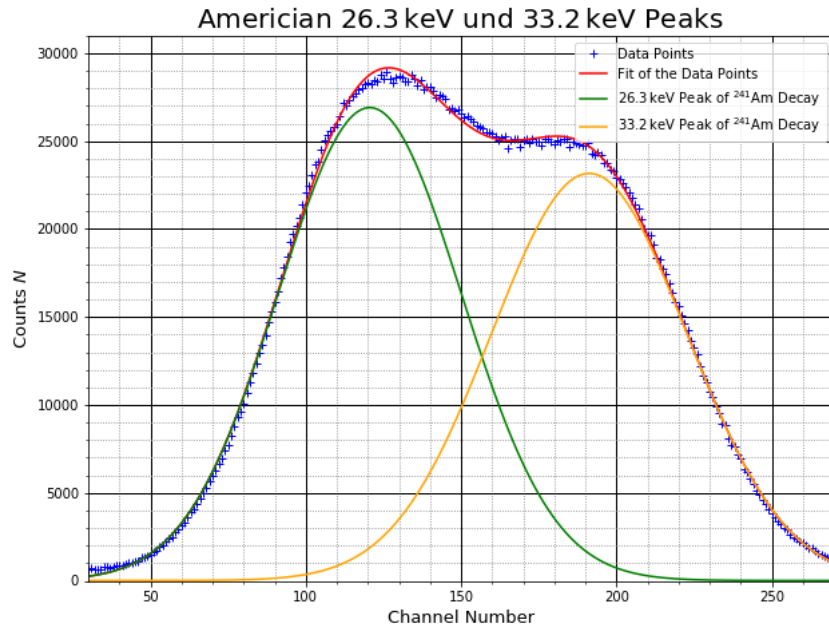
Figure 13: Measured Americium Energy Spectra of the 26.3 keV and 33.2 keV double peak with fits of the split peaks. Spectrum of the left scintillator.
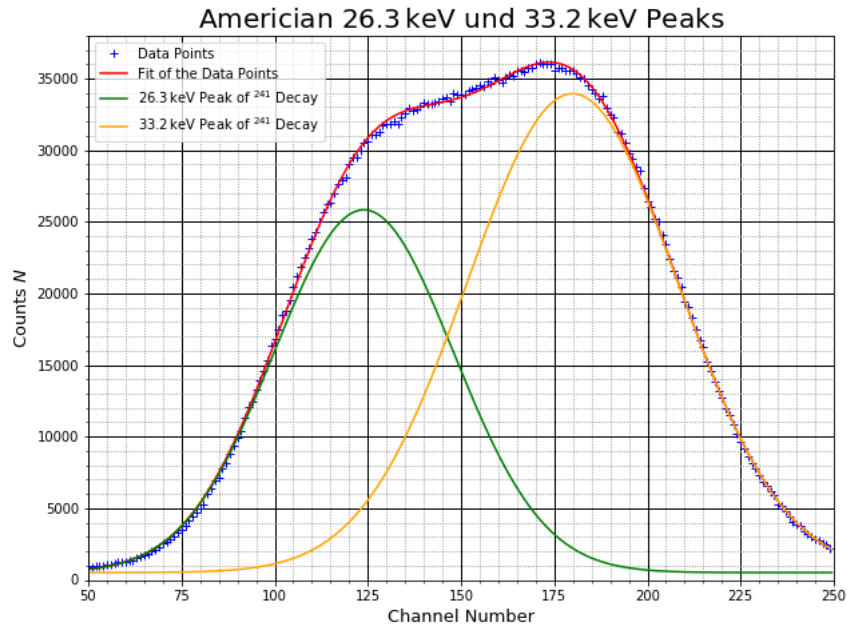
Figure 14: Measured Americium Energy Spectra of the 26.3 keV and 33.2 keV double peak with fits of the split peaks. Spectrum of the right scintillator.

4.4 Analysis of the delayed coincidences measurement

4.4.1 Time calibration

To correctly compute the half-live of the 14.4 keV state of ^{57}Fe, the conversion of time difference to the channels in the MCA is determined. The data collected for this purpose is found in the appendix. The channel and delay pairs were plotted and a unweighted linear model of first order was fitted to the data. The plot is shown in figure 15. The fitted linear model had the form of $n(\Delta t) = m \cdot \Delta t + c$. To calculate the parameters of the fit the python package `scipy.optimize.curve_fit`[3] was used. The fitted parameters were:

$$m = (1.2 \pm 0.007) \frac{1}{\text{ns}}$$

$$c = (-21.5 \pm 0.7)$$

The error for the time was estimated to be ± 0.5 ns, which is too small to be visible in the graphic. This parameters were used to compute the time corresponding to each channel using formula 7. x_{cal} represents the calibrated value, x_{norm} the original value.

$$x_{\text{cal}} = \frac{x_{\text{norm}} - c}{m} \tag{7}$$
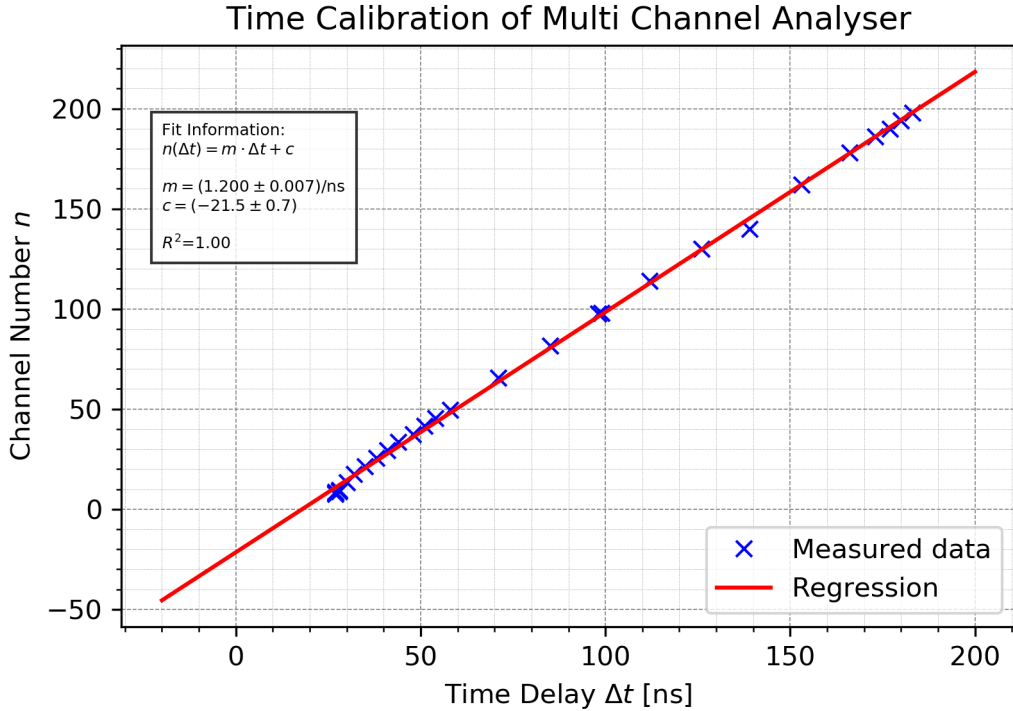
Figure 15: Plot of the datapoints of the time calibration and the linear fit of them. The errors are too small to be visible in the graphic.

4.4.2 Analysis on linear scale

For the analysis in the linear scale, two ranges of the data set were chosen. One was used for the background compensation, the other one for the exponential fit. For a visual representation and the exact value ranges, see figure 16. The error on the counts is, because a poisson distribution was assumed, computed by equation 8. s_{counts} is the error for the counts of a channel, n the actual counts of the same channel. All errors were calculated for each channel individually.

$$s_{\text{counts}} = \sqrt{n} \tag{8}$$
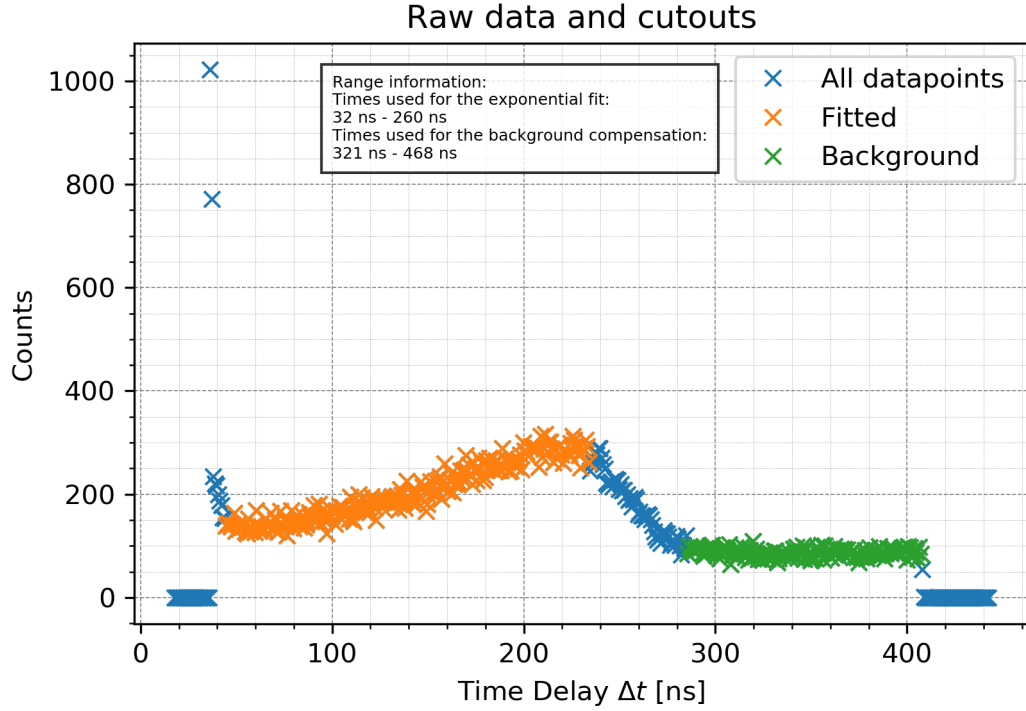
Figure 16: Plot of the datapoints with corrected time. The ranges of the data used for each different regression are marked in the graphic. The start and endpoints for each range are also given.

As the next step a curve, analog to the one used for the time calibration, was fitted to the range designated for the background compensation. A visual representation of this fit is given in figure 19. This fitted curve was then subtracted from all the datapoints, as a mean to reduce the influence of random background coincidences. The reason why the green part in figure 16 can be used is that for the part of our measurement the random coincidences is almost flat. This is due to the fast decay of $9ns$ of our 136.5 keV state. Since it decays so fast the measurement takes part in the flat area of the background. To get the curve for the background we fit the Data Points using the python package `scipy.optimize.curve_fit` [3]. The parameters for the curve in form of $f(x) = m \cdot x + c$ are:

$$m = (-0.015 \pm 0.020)\frac{1}{\text{ns}}$$
$$c = (92 \pm 7)$$

After subtracting the background coincidences, a exponential function of the form 9 was used to approximate the value of the decay constant b in the fit. The parameter b in figure 17 is the decay constant of our state.

$$y(x, a, b, c, d) = a \cdot \exp(b \cdot (x + d)) + c \tag{9}$$

To get the half life the eq.10 can be used as well as eq.11 to calculate the error.

$$T_{\frac{1}{2}} = \frac{\log(2)}{b} \tag{10}$$

$$\Delta_T = \frac{\log(2)}{b^2} \tag{11}$$

With that the half life is $T_{\frac{1}{2}} = (83 \pm 9952)\,\text{ns}$.

4.4.3 Analysis on logarithmic scale

For the analysis on the logarithmic scale, the ln of every count value and their respective error was computed. This data and its errors are illustrated in figure 18. Following this, almost the same steps as in the analysis on the linear scale were carried out. Starting with a linear fit in the background data

14
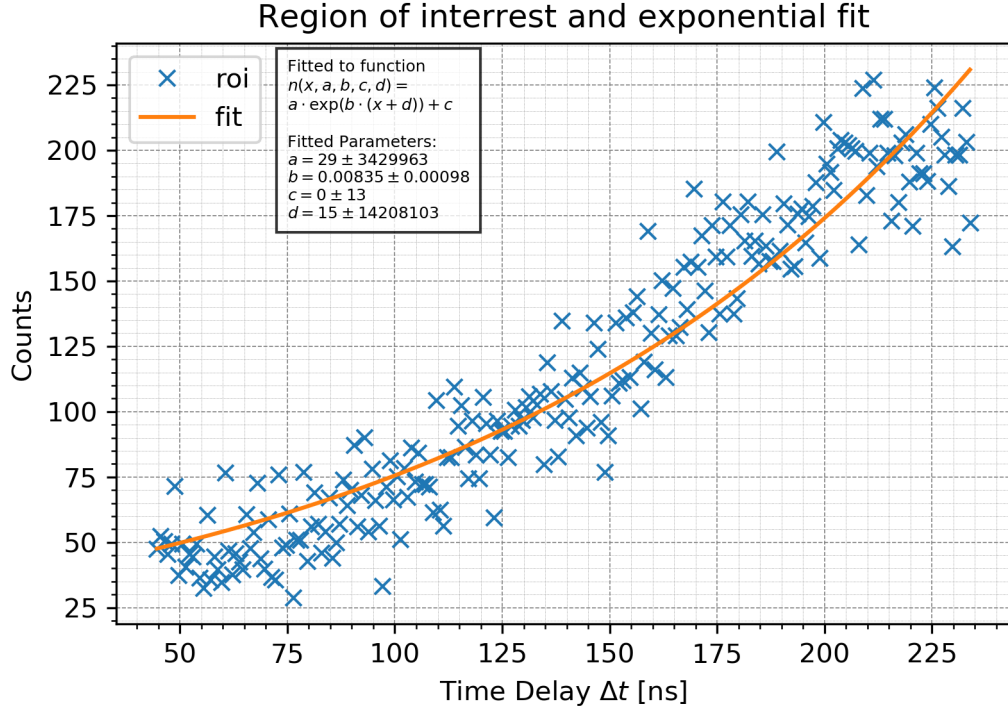
Figure 17: Plot of the datapoints in the roi with the fitted exponential curve. The determined parameters are given in the picture.

range (fig. 20), the background was subtracted from the original logarithmic data (fig. 21). The main difference of this part was the linear fit in the region of interest (fig. 22).

Utilizing the slope of the fitted curve to the region of interrest, an other value for the half life of the 14.4 keV state of ^{57}Fe was computed.

$$b_{\log} = (0.005 \pm 0.004)$$

Utilizing formulas 10 and 11, the half life was determined.

$$T_{\frac{1}{2}\log} = (142 \pm 3)\,ns$$

Figure 18: Logarithmic scaled plot all data points. Notable are the abnormally big errors.

5 Discussion

5.1 Delayed coincidences

Prominent for the delayed coincidence measurement is, that no extra background coincidence measurement was conducted. This is due to the extra channels after the decay peak of the 14.4 keV state of ^{57}Fe. This also provided a very accurate background measurement, due to its long duration.

The guessed error from the times for the time calibration measurement seems in retrospective appropriate. Although it seemed too small at during the experiment, the fitted curve shows aligns very good with the data points.

Notable for the linear scaled fit for the decay peak were multiple things. First the slightly descending slope of the curve fitted to the background data. This is a indication of the fast decaying 136.5 keV state of ^{57}Fe, where some of the background coincidences originate from.

Second to this is the fact, that the range used for the exponential fit greatly influence the resulting fitted parameter. If extended far enough, one could fit the perfect literature value of the half life of the 14.4 keV

state. The computed half life with this method is close to the literature value of 98 ns. Using the formula 12, the compatibility of both is 0.0014.

$$t = \frac{|\text{compared value} - \text{literature value}|}{\text{uncertainty/error of compared value}} \tag{12}$$

This good compatibility is caused by the extremly large error of the computed half live. The method, used to compute this error is probably faulty, or the computation itself has an error.

With logarithmic scaled fit has multiple problems. The two most obvious ones are the incorrect error computations resulting in, by comparison, large errors. The errors are also symmetric, which should not happen in a logarithmic plot. Unfortunately, due to the advanced time, this could not be fixed. The second big problem lies with the alomost 1.5 times too great computed half life of the logarithmic plot. Some of it can be explained by choosing the wrong range of values to fit, but this can not be the only explanation. The error on this value as unrealistic as the one from the linear plot, resulting in the same good compatibility of 0.0015. For this is also the only explanation a wrong error computation formula.

6 Bibliograpy

References

[1] *Versuchsanleitung: Fortgeschrittenen Praktikum Teil 1 Kurze Halbwertszeiten.*

[2] E. Bodenstedt. *Experimente der Kernphysik und ihre Deutung, Teil 2.* Bibliographisches Institut, 1978.

[3] Eric Jones, Travis Oliphant, Pearu Peterson, et al. Python3 package `scipy.optimize` for curve fitting., 2001–.

7 List of tables

List of Tables

8 List of Figures
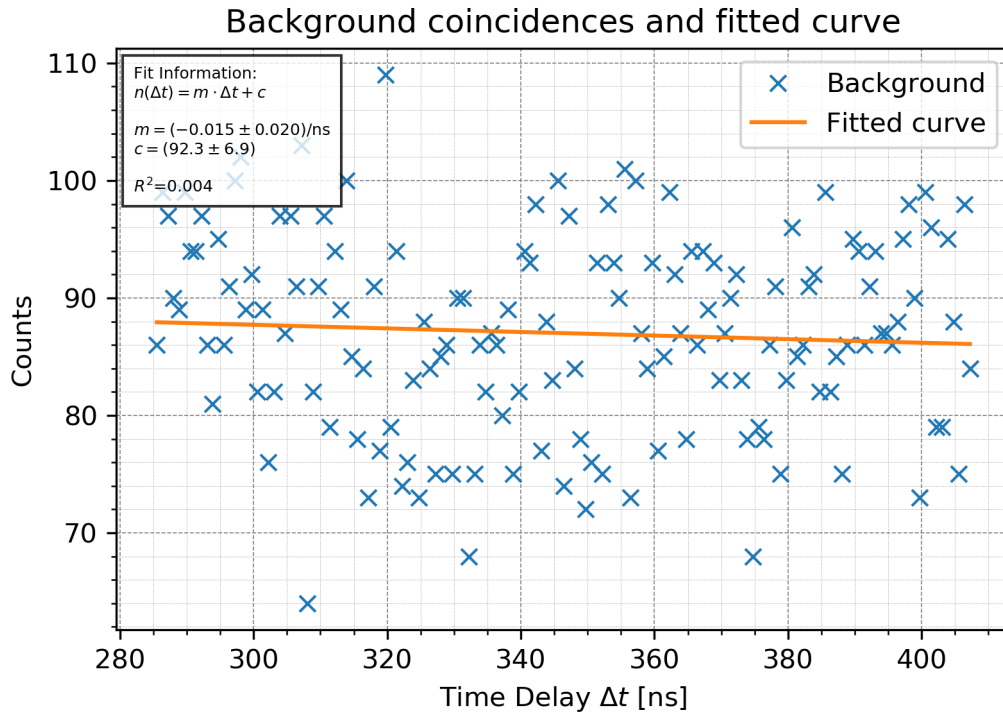
List of Figures

9   Appendix

Figure 19: Plot of the datapoints with corrected time. The ranges of the data used for each different regression are marked in the graphic. The start and endpoints for each range are also given.

Figure 20: Logarithmic scaled plot of the background data with the fitted curve. Notable are the abnormally big errors.

Figure 21: Logarithmic scaled plot of all data with subtracted background curve. Due to the choice of the axis labels, some of the unused data is not visible. Notable are the abnormally big errors.

Figure 22: Logarithmic scaled plot of the region of interest and the fitted curve. Notable are the abnormally big errors.